Journal of Materials Chemistry A

Accepted Manuscript

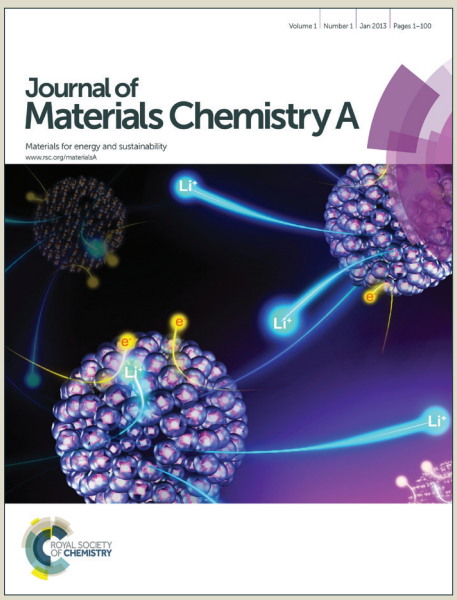

ROYAL SOCIETY OF CHEMISTRY

www.rsc.org/materialsA

Journal Name

ARTICLE

A novel solid-state electrolyte based on crown ether lithium salt complex

Received 00th January 20xx,
Accepted 00th January 20xx

DOI: 10.1039/x0xx00000x

www.rsc.org/

Minda Gao, Yun Wang, Qinghua Yi, Ying Su, Pengfei Sun, Xiangguo Wang, Jie Zhao* and Guifu Zou*

A novel crown ether lithium salt complex [Liϵ12-C-4][I] has been designed, synthesized and characterized. The thermal properties of [Liϵ12-C-4][I] based solid-state electrolytes are also investigated in detailed. The particularly trapping ability of 12-crown-4 to Li^+ can obviously reduce the cation-anion (Li^+-I^-) interaction and hence facilitate favorable electrical properties of the solid-state electrolytes. Therefore, Liϵ12-C-4][I] represents ionic conductivity of 3.93×10^{-5} and 1.53×10^{-4} S cm^{-1} at 25 and 80 ^{o}C, respectively. Further addition of an ionic liquid 1-propyl-3-methylimidazolium iodine as a crystal growth inhibitor could effectively suppress the crystallization of the complex for more amorphous and smoother regions, which are much more facile for higher ion conductivity by the segmental motion of molecule chains. As an application, the resulting device shows a power conversion efficiency of 5% and displays excellent long-term stability. These results offer us more opportunities to explore simple and novel solid-state electrolytes for energy storage and conversion.

1. Introduction

In most electrochemical devices, electrolytes are a kind of ubiquitous and indispensable materials. Due to their outstanding dissolvability to inorganic and organic compounds, large dielectric coefficients to dissociate inorganic salts and feasible permeability across the electrodes, electrolytes have been supposed as highly promising mediums facilitating the transfer of charges (e.g. H^+, Li^+ and I^-) for renewable energy devices.[1-3] However, organic liquid/gel electrolytes containing organic solvent often suffer from serious drawbacks caused by volatilization, leakage, flammability and electrode corrosion,[3,4] restraining the long-term stability and practical security of their devices. In this regard, solid-state electrolytes have attracted great attention for an extended research interest. For example, Bruce' group developed a series of polymer electrolytes by dissolving $LiXF_6$ (X=P, As, Sb) in polyethylene oxide (PEO).[5,6] These new polymer electrolytes could remain around 10^{-5} S cm^{-1} at room temperature, displaying their potential use in rechargeable lithium batteries. Bouchet and coworkers[7] designed a multifunctional single-ion polymer electrolyte based on polyanionic block copolymers comprising polystyrene segments. Ionic conductivity ~1.3×10^{-5} S cm^{-1} at 60 ^{o}C, high Li^+ transport number (>0.85) and improved mechanical strength rendered the electrolyte to be a new class of macromolecular material for lithium-metal battery. In dye-sensitized solar cells, overall photoelectric conversion efficiency over 13% has been achieved by embedding cobalt redox shuttles into an organic liquid electrolyte.[8] However, dye degradation, leakage and evaporation of organic solvent, and electrode corrosion restrain the long-term performance for their practical applications.[3] Therefore, several methods, including p-type semiconductors[9] and hole conductors,[10,11] especially polymer electrolytes, have been proposed to overcome these drawbacks.[12-15] Unfortunately, because of lower conductivity and imperfect soakage of porous electrodes for polymer electrolytes, it is still a big challenge to improve the ion dynamics and permeability.[3,4,16,17] Impressively, small molecular based solid-state ionic conductors provide higher ion conductivity, better solution-processable property and more satisfactory contact between the electrolytes and electrodes, highlighting their widespread application in fuel cells,[20] lithium batteries[18-19] and dye-sensitized solar cells.[21-24] Therefore, new solid-state electrolytes offer more opportunities to demonstrate their basic research interest and extensively promising applications in energy storage and conversion fields.

Here, we design and synthesize a simple solid-state electrolyte based on crown ether lithium salt complex ([Liϵ12-C-4][I]) by mixing liquid-state 12-crown-4 with lithium iodide. The chemical structure and thermal properties are confirmed and characterized using a range of technologies including Fourier transform infrared (FTIR) spectra, nuclear magnetic resonance (NMR) measurement, X-ray diffraction (XRD) patterns and differential scanning calorimetry (DSC) analysis. The thermal properties, ion conductivity, surface morphology of [Liϵ12-C-4][I] based solid-state electrolytes are also

College of Physics, Optoelectronics and Energy & Collaborative Innovation Center of Suzhou Nano Science and Technology, Soochow University, Suzhou215006, P.R. China. E-mail: jzhao@suda.edu.cn; zouguifu@suda.edu.cn

† Electronic Supplementary Information (ESI) available: [details of any supplementary information available should be included here]. See DOI: 10.1039/x0xx00000x

investigated. As an application, the solid-state electrolytes are further used to fabricate dye-sensitized solar cells (DSSCs).

2. Experimental

Materials

12-Crown-4, lithium iodide (LiI) and iodine (I_2) were purchased from Alfa Aesar and used as received. PMII was purchased from Merck. H_2PtCl_6 and organic dye Z-907 were purchased from Aldrich. All the chemical reagents were used without further treatment. Fluorine-doped tin oxide (FTO) glass electrodes (8 Ω/Sq), and slurries containing 20 nm-sized mesoporous and 200 nm-diameter light-scattering TiO_2 colloidal were purchased from Dalian Hepat Chroma Solar Tech. Co., Ltd (China).

Synthesis of [Liϵ12-C-4][I]

[Liϵ12-C-4][I] was synthesized as follows: briefly, a mixture of 12-crown-4 (31 mmol, 5.46 g) and LiI (30 mmol, 4.02 g) in 20 mL ethanol was stirred at 50 °C for 12 h under a nitrogen atmosphere. After the evaporation of solvent, the excessive 12-crown-4 was further removed by vacuum distillation at 80 °C. The product was dried under vacuum at 80 °C for 24 h to produce [Liϵ12-C-4][I] with a yield of 98%.

Preparation of [Liϵ12-C-4][I] based solid-state electrolytes

The components of the solid-state electrolytes employed in this work are listed in Table 1. All the electrolytes were dried under vacuum at room temperature for 48 h before the characterization and fabrication for DSSCs. The thermal stability of Sample A (12-crown-4) and Electrolyte B ([Liϵ12-C-4][I]) is tested by TGA. For DSC analysis, Sample A and Electrolytes B-G containing different contents of PMII are also measured. Since I_2 is needed to form I_3^- ions for electron relay at the counter electrode, addition of 20 wt% I_2 to Electrolyte B can obtain Electrolyte I for the fabrication of DSSCs. Moreover, containing Electrolyte I and 200 wt% PMII, Electrolyte J is also prepared. For comparison, a typical organic liquid electrolyte for Reference Device contains 0.6 M DMPII, 0.1 M LiI, 0.5 M TBP, 0.1 M I_2 in MPN.[33,34]

Table 1 The components, property and conductivity of [Liϵ12-C-4][I] based solid-state electrolytes.

Sample/ Electrolyte	12-crown-4	LiI	PMII (wt%)	I_2 (wt%)	State[a]	Mp (°C)[b]	Conductivity (10^{-5} S cm^{-1})[c]
A	√	—	—	—	Liquid	19.8	—
B	√	√	—	—	Solid	64	3.93
C	√	√	20	—	Solid	64	4.76
D	√	√	30	—	Solid	64	5.89
E	√	√	40	—	Solid	64	6.93
F	√	√	100	—	Solid	64	11.24
G	√	√	200	—	Solid	64	15.77
I	√	√	—	20	Solid	64	12.53
J	√	√	200	20	Solid	64	39.64

[a] The state of electrolytes is present at 25 oC. [b] Melting point tested by DSC. [c] Tested by EIS at 25 °C. [—] No addition or no measurement.

Device Fabrication

The fabrication of DSSCs was assembled as documented in the previous literature.[21] The cleaned FTO glass was covered at two parallel edges with an adhesive tape to control the thickness of mesoporous TiO_2 film. Two layers of TiO_2 particles were deposited onto cleaned FTO glass and used as photoelectrodes. A 10 µm thick film of 20 nm sized TiO_2 particles was deposited onto the FTO glass electrode by the doctor-blade technique. The film was dried at 125 °C for 5 min. Then, a second 5 µm thick layer of 200 nm light-scattering anatase particles were coated on the top of the first TiO_2 layer. The resulting TiO_2 films were annealed at 500 °C for 15 min. After cooling to 80 °C, the obtained TiO_2 electrode was immersed in 0.3 mM solution of MK-2 in anhydrous toluene at room temperature for 12 h. The dyed TiO_2 electrode was washed with anhydrous ethanol and dried with nitrogen stream. To prepare the Pt counter electrode, two drops of 5 mM H_2PtCl_6 in ethanol was placed onto the cleaned FTO glass substrate, followed by drying and annealing at 400 °C for 15 min.

DSSCs were fabricated by sandwiching the methanol solution of an electrolyte between a dye-sensitized TiO_2 electrode and a pre-drilled Pt counter electrode by a 40 µm hot melt ring (Surlyn, DuPont). The resulting cells were placed in vacuum at 50 °C for overnight to remove air to guarantee optimum filling and fine electrical contact. The produced devices were sealed with a Surlyn sheet and a thin glass cover by heating.

Characterization and Measurement

^{1}HNMR spectra were recorded on a Varian 400 MHz spectrometer. Fourier transform infrared (FTIR) spectra of the synthesized compounds were recorded on a Varian CP-3800 spectrometer in the range of 4000-400 cm^{-1}. Thermal analysis was carried out on Universal Analysis 2000 thermogravimetric analyzer (TGA). Samples were heated from 50 to 500 °C at a heating rate of 10 °C min^{-1} under a nitrogen flow. Differential scanning calorimetry (DSC) measurements were performed under a nitrogen atmosphere with a heating rate of 10 °C min^{-1} in a temperature range of -50 to 200 °C on DSC-Q200.

The XRD patterns of the films were performed by Riguku D/MAX-2000PC diffraction system to evaluate the crystal structure and lattice constants, with a diffraction angle 2θ ranging from 5° to 80°. According to equation (1), the interlayer distances between planes in the atomic lattice can be calculated.

$$2d\sin\theta = n\lambda \quad (1)$$

where λ is the wavelength (= 0.154 nm) of the incident beam, θ is the angle between the incident ray and the scattering plane, and n is an integer.

The conductivity of electrolytes was characterized between two identical platinum sheets (diameter of 1 cm) on a CHI660c electrochemical workstation, using the AC impedance method over the frequency range 0.01 Hz to 10^5 Hz and the amplitude is 10 mV. The conductivity was calculated using equation (2):[17,21-23]

$$\sigma = \frac{l}{RS} \quad (2)$$

where σ is the conductivity in S cm^{-1}, R is the ohmic resistance of the electrolyte, l is the distance between two electrodes, and S is the area of the electrolyte.

All the samples were equilibrated for at least 20 min at a given temperature. The photocurrent density-voltage (J-V) curves of the assembled DSSCs shielded by an aluminum foil mask with an aperture area of ~0.25 cm^2 were measured with a digital source meter (Keithley, model 2612) under simulated air mass (AM) 1.5 solar spectrum illumination at 100 mW cm^{-2}. Incident photo-to-current conversion efficiency (IPCE) plotted as a function of excitation wavelength was recorded on a Keithley 2612 source meter under the irradiation of a Xenon lamp with a monochromater (Oriel CornerstoneTM 260 1/4). The photoelectrochemical parameters, such as short-circuit current density (J_{sc}), open-circuit voltage (V_{oc}), fill factor (FF) and power conversion efficiency (PCE) were calculated according to the previous reports.[3,4,16,17]

3. Results and discussion

Crown ethers are a class of heterocycles with cyclic oligomers of essential repeating ethyleneoxy (-CH_2CH_2O-).[25] The unique structure of cyclic dioxanes renders crown ethers as complexing agents to effectively bind alkali-metal cations[26] and reduce the interaction strength of their ion pairing.[27] Up to now, crown ethers have been widely used in size-selective ions sensors,[25,28] phase-transfer catalysts,[29] membrane transports[30] and disposals of nuclear waste.[31] As one of simple crown ethers, 12-crown-4 repeats twice in dioxane and four times in its structure. The cavity radius of 12-crown-4 is between 0.060 and 0.075 nm, while the ionic radius of Li+ is 0.060 nm.[32,35] The excellent trapping and dissociating ability of 12-crown-4 to Li^+ from its counterions triggers our interest in further exploring the possibility to fabricate a solid-state electrolyte based on [Liϵ12-C-4][I], which could free out I^- ions and facilitate their effective transfer of charges.

Fig. 1a shows the synthetic route and chemical structures of [Liϵ12-C-4][I]. The purity and chemical structures are confirmed by ^{1}HNMR (Fig. S1-S2, ESI†). Compared with the single peak at 3.71 ppm for 12-crown-4 in $CDCl_3$ (Fig. S1, ESI†), introducing LiI will lead to three split peaks at 3.86, 3.83 and 1.25 ppm (Fig. S2, ESI†), probably because of non-planar/asymmetric structure of [Liϵ12-C-4][I]. In addition, as shown in Fig.S3, XRD measurements can provide insight into the molecular packing arrangement. The Bragg peaks of 2θ are clearly observed at 20.88 and 18.18° for LiI and [Liϵ12-C-4][I], respectively. According to the equation (1), the interlayer distances between planes in the atomic lattice can be calculated to be 4.25 and 4.87 Å for LiI and [Liϵ12-C-4][I], respectively. It means that synthesized [Liϵ12-C-4][I] exhibits a larger interlayer distance than LiI. The dissociating and partition ability of 12-crown-4 ring to LiI should be probably responsible for this analysis. Furthermore, representative images of electrolytes are also shown in Fig. 1b. Impressively, introducing LiI into clearly liquid 12-crown-4 (Sample A) results in pale-yellow power (Electrolyte B), indicating effective interaction between oxygen atoms and lithium ion to form [Liϵ12-C-4][I]. Further addition of I_2 could obtain Electrolyte I containing small crystals with a purple color. It is notable that adding PMII into Electrolytes B and I could effectively suppress the crystallization of the complex to form Electrolytes G and J, which will be further discussed by DSC and SEM.

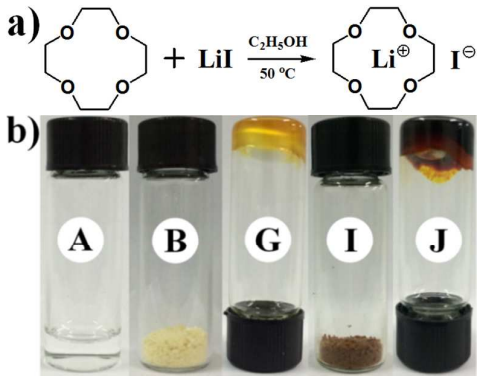

Fig. 1 (a) Synthetic procedures for the preparation of [Liϵ12-C-4][I]. (b) Typical photographs of Sample A, Electrolytes B, G, I and J at 25 °C, respectively.

The thermal stability of 12-crown-4 and [Liϵ12-C-4][I] is also studied in Fig. 2. It can be found that the initial decomposition temperature (T_{onset}) of 12-crown-4 is lower than 100 °C, indicative of poor thermo-stability. Notably, [Liϵ12-C-4][I] represents much higher excellent thermo-stability with a T_{onset} of 280 °C. Meanwhile, taking account of carbon residue, the adding amount of LiI to 12-crown-4 is further confirmed by residue mass fraction ~43.38%, in accordance with the theoretical value of 43.17% for [Liϵ12-C-4][I]. These results indicate that synthesized [Liϵ12-C-4][I] indeed offers a high thermal stability, far beyond the range of interest for solid-state electrolytes.

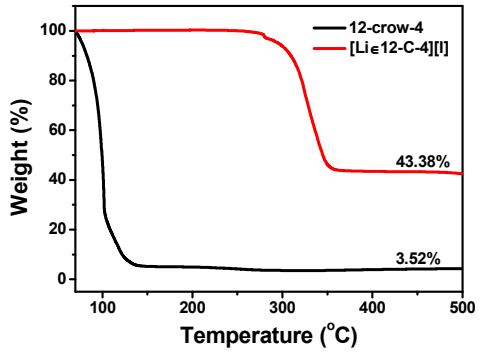

Fig. 2 TGA curves of 12-crown-4 and [Liϵ12-C-4][I].

In order to further investigate the thermal property of Sample A and Electrolytes B-G, DSC curves are shown in Fig. 3. The state and melting points are also summarized in Table 1. It can be found that the melting point of Sample A is 19.8 °C, whereas, it exhibits a colorless liquid at room temperature (Fig. 1b). Notably, Electrolyte B containing [Liϵ12-C-4][I] represents pale-yellow power (Fig. 1b) with a Mp of 64 °C, indicating strong interaction between 12-crown-4 and LiI. The influence of adding I_2 on the melting point of Electrolyte I is also shown in Fig. S4. The value of 64.6 °C indicates that adding I_2 can lead to slightly higher Mp than that of Electrolyte B, due to enhanced van der Waals interactions of polyiodide.[16] Compared with Electrolyte B, adding 20 to 40 wt% of PMII for Electrolytes C-E will result in slightly reduced intensity of the melting point. Further addition of PMII from 100 to 200 wt% can obviously decrease its intensity. These results demonstrate that liquid state PMII can effectively restrain the crystallization of [Liϵ12-C-4][I] and thus introduce the appearance of defected/amorphous regions (Fig. 5b),[36-38] which is favorable for better ion conductivity from 3.93×10^{-5} to 1.58×10^{-4} S cm^{-1} shown in Table 1. However, various addition of PMII has little effect on the Mp values of prepared solid-state electrolytes. The solid-state property of crown ether lithium salt complex is also in accordance with the range of application interest for solid-state electrolytes.

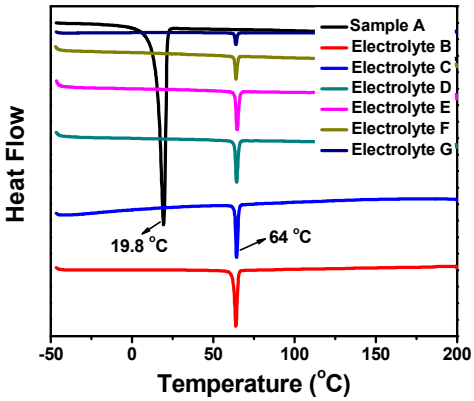

Fig. 3 The DSC curves for Sample A and Electrolytes B-G, respectively.

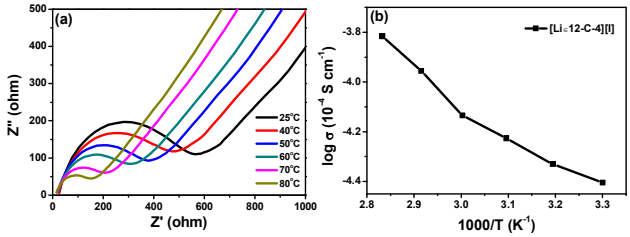

Fig. 4 AC impedance spectra (a) and ionic conductivity (b) as a function of temperature for synthesized [Liϵ12-C-4][I].

As shown in Fig. 4, the AC impedance spectra and ionic conductivity tests as a function of temperature are carried out to study the influence of temperature (25-80 °C) on the electrochemical performance of synthesized [Liϵ12-C-4][I]. The conductivity is 3.93×10^{-5} S cm^{-1} at 25 °C. It can been seen that temperature increment would gradually reduce the impedance values and hence enhance the ionic conductivity of [Liϵ12-C-4][I]. Because of its melting point at 64 °C, higher temperature will exhibit a liquid state of [Liϵ12-C-4][I], resulting in obvious enhancement of ionic conductivity. Therefore, the solid-state electrolyte shows an ionic conductivity ~1.53×10^{-4} S cm^{-1} at 80 °C, displaying potential application as a novel ionic conductor.

As shown in Fig. 5, the surface morphologies of synthesized [Liϵ12-C-4][I] and PMII doped [Liϵ12-C-4][I] are further investigated. It can be found that [Liϵ12-C-4][I] is prone to crystallize and form voids at ambient condition (Fig. 5a). The sizes of formed crystals are about 5-10 μm. However, crystallization and voids can greatly prevent the filling of solid-state electrolytes into porous TiO_2 films, which will increase internal resistance between electrodes and electrolytes, and hence destroy dye regeneration and photocurrent generation (e.g. DSSCs).[39-41] Therefore, liquid state PMII as an crystal growth inhibitor can effectively restrain the crystal growth of [Liϵ12-C-4][I], leading to relatively smooth surface morphology and improved interfacial wetting property (Fig. 5b). For these reasons, electrolytes with smooth surface morphology will be probably favorable for the fabrication of solid-state DSSCs in this work.

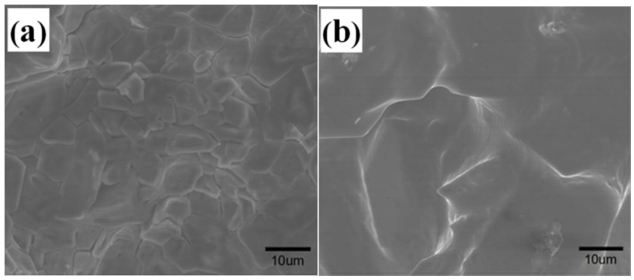

Fig. 5 SEM images of [Liϵ12-C-4][I] (a, Electrolyte B) and 200 wt% PMII doped [Liϵ12-C-4][I] (b, Electrolyte G) coated on dyed TiO_2 photoanodes.

Based on the abovementioned analysis, Electrolytes B, G, I and J are chosen for the fabrication of solid–state DSSCs (Device I-IV). The J-V curves of Device I and II with I_2 are shown in Fig. 6a. Meanwhile, The J-V curves of Device I and II without I_2 are also shown in Fig. S5 in ESI. Device III without I_2 exhibits a PCE of 1.04 % (J_{sc} = 3.74 mA cm^{-2}, V_{oc} = 0.525 and FF = 0.502). For Device I, because of the function of I_2 to form I_3^- ions for effective dye regeneration, the values of J_{sc}, V_{oc}, and FF are 5.02 mA cm^{-2}, 0.567 V and 0.669, yielding a PCE of 1.90 %. Due to special structure and relatively higher ionic conductivity of [Liϵ12-C-4][I], the PCE is better than those of solid-state electrolytes in previous reports.[39,41,42] However, as shown in Fig. 5a, large crystallization and formed voids can greatly prevent the filling of solid-state electrolyte into the TiO_2 pores.

Meanwhile, poor interfacial contact between photoanode and electrolyte also hinder the dye regeneration and ion transport, and hence reduced photocurrent generation. With the assistance of the crystal growth inhibitor PMII to [Liϵ12-C-4][I], as shown in Fig. 6a and Fig. S5, the PCEs of Device IV without I_2 and Device II with I_2 can be remarkably improved to 2.77% (J_{sc} = 9.12 mA cm^{-2}, V_{oc} = 0.604 and FF = 0.502) and 5.05% (J_{sc} = 11.57 mA cm^{-2}, V_{oc} = 0.627 and FF = 0.696), respectively. This can be ascribed to much more smooth surface morphology, better interfacial contact, higher ionic conductivity and more effective dye generation. Although the efficiency is slightly lower than that of Reference Device with a PCE of 5.72%, it also indicate comparative performance of [Liϵ12-C-4][I] based device. These results are further demonstrated by IPCE testing shown in Fig. 6b. The maximum IPCE values are 42.51, 78.72 and 81.4% at 530 nm, indicating high light harvesting efficiency, effective dye regeneration and charge collection for photoelectron conversion efficiencies.

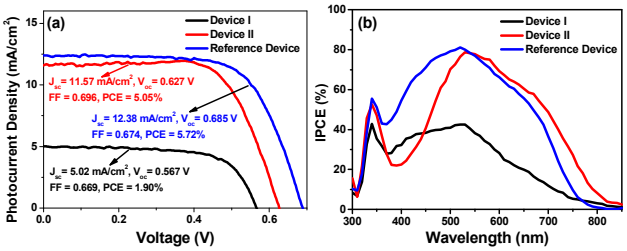

Fig. 6 (a) J-V curves and (b) IPCE *vs*. wavelength profiles for solid-state DSSC based on Electrolytes I and J, respectively. A typical organic liquid electrolyte for Reference Device contains 0.6 M DMPII, 0.1 M LiI, 0.5 M TBP, 0.1 M I_2 in MPN.[33,34]

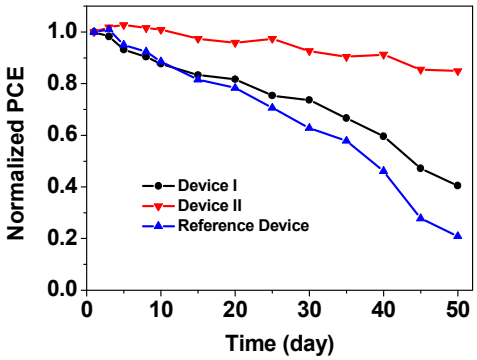

Fig. 7 Time-course variation of normalized PCE for the fabricated solid-state DSSCs with successive one sun light soaking during the accelerated aging test at 60 °C.

As shown in Fig. 7, the long-term stabilities of abovementioned Device I and II, and Reference Device are further investigated at 60 °C under the same condition. During this period, Device I containing Electrolyte I shows gradual decrease of PCE. After the aging test of 50 days, Device I maintains only about 40% of its initial conversion efficiency because of the crystallization and voids of [Liϵ12-C-4][I]. However, as expected, Device II remains almost over 85% of its initial conversion efficiency, indicating much better excellent stability than Device I. Employing PMII to overcome the disadvantages of [Liϵ12-C-4][I] crystallization for Electrolyte J should be responsible for the stability enhancement. For comparison, the Reference Device with an organic liquid electrolyte maintains only about 20% of its initial conversion efficiency. These results also offer us a feasible method to design novel solid-state electrolytes for high performance DSSCs for future practical applications.

4. Conclusions

In summary, a simple and novel crown ether lithium salt complex [Liϵ12-C-4][I] has been designed, synthesized and characterized with high purity and yield. The thermal behaviors of [Liϵ12-C-4][I] based solid-state electrolytes are also investigated in detailed. It reveals that molecule interaction between crown ether and lithium iodide can effectively transform liquid state 12-crown-4 to form solid-state complex [Liϵ12-C-4][I] with a melting point at 64 °C, which is in the range of interest for solid-state electrolytes. Particularly, the trapping ability of 12-crown-4 to Li+ can obviously reduce the cation-anion (Li^+-I^-) interaction and hence facilitate favorable electrical properties of the solid-state electrolytes. Therefore, Liϵ12-C-4][I] represents ionic conductivity of 3.93×10^{-5} and 1.53×10^{-4} S cm^{-1} at 25 and 80 °C, respectively. Further addition of PMII could effectively suppress the crystallization of the complex for more amorphous and smoother regions, which are much more facile for higher ion conductivity by the segmental motion of molecule chains. Therefore, the resulting device shows a PCE ~5% and displays excellent long-term stability. These results offer us more opportunities to explore simple and novel solid-state electrolytes for electrochemical devices.

Acknowledgements

This work was supported by “973” Program-the National Basic Research Program of China" Special Funds for the Chief Young Scientist (2015CB358600), the Excellent Young Scholar Fund from National Natural Science Foundation of China (21422103), Jiangsu Fund for Distinguished Young Scientist (BK20140010), the Natural Science Foundation of Jiangsu Province (No. BK20140311), University Science Research Project of Jiangsu Province (No. 13KJB150033), the Open Foundation of Jiangsu Key Laboratory of Thin Films and the Project Funded by the PAPD of Jiangsu Higher Education Institutions.

Notes and references

1 H. W. Zhang and P. K. Shen, *Chem. Rev.*, 2012, **112**, 2780-2832.
2 K. Xu, *Chem. Rev.*, 2004, **104**, 4303-4417.

3 J. H. Wu, Z. Lan, J. M. Lin, M. L. Huang, Y. F. Huang, L. Q. Fan and G. G. Luo, *Chem. Rev*., 2015, **115**, 2136–2173.
4 J. L. Nei de Freitas, A. F. Nogueira and M-A. De Paoli, *J. Mater. Chem*., 2009, **19**, 5279–5294.
5 Z. Gadjourova, Y. G. Andreev, D. P. Tunstall and P. G. Bruce, *Nature*, 2001, **412**, 520-523.
6 A. M. Christie, S. J. Lilley, E. Staunton, Y. G. Andreev and P. G. Bruce, *Nature*, 2005, **433**, 50-53.
7 R. Bouchet, S. Maria, R. Meziane, A. Aboulaich, L. Lienafa, J. P. Bonnet, T. N. T. Phan, D. Bertin, D. Gigmes, D. Devaux, R. Denoyel and M. Armand, *Nat. Mater*., 2013, **12**, 452-457.
8 S. Mathew, A. Yella, P. Gao, R. Humphry-Baker, B. F. E. Curchod, N. Ashari-Astani, I. Tavernelli, U. Rothlisberger, M. K. Nazeeruddin and M. Grätzel. *Nat. Chem*., 2014, **6**, 242-247.
9 K. Tennakone, G. Senadeera, D. De Silva and I. Kottegoda, *Appl. Phys. Lett*., 2000, **77**, 2367-2369.
10 U. Bach, D. Lupo, P. Comte, J. Moser, F. Weissörtel, J. Salbeck, H. Spreitzer and M. Grätzel, *Nature*, 1998, **395**, 583-585.
11 C. S. Karthikeyan, H. Wietasch and M. Thelakkat, *Adv. Mater*., 2007, **19**, 1091-1095.
12 H. Han, W. Liu, J. Zhang and X. Z. Zhao, *Adv. Funct. Mater*., 2005, **15**, 1940-1944.
13 M. Biancardo, K. West and F. C. Krebs, *Sol. Energy Mater. Sol. Cells*, 2006, **90**, 2575-2588.
14 J. Xia, N. Masaki, M. Lira-Cantu, Y. Kim, K. Jiang and S. Yanagida, *J. Am. Chem. Soc*., 2008, **130**, 1258-1263.
15 J. Nei de Freitas, A. F. Nogueira and M. A. De Paoli, *J. Mater. Chem*., 2009, **19**, 5279-5294.
16 J. H. Wu, S. C. Hao, Z. Lan, J. M. Lin, M. L. Huang, Y. F. Huang, P. J. Li, S. Yin and T. Sato, *J. Am. Chem. Soc*., 2008, **130**, 11568–11569.
17 J. M. Pringle, P. C. Howlett, D. R. MacFarlane and M. Forsyth, *J. Mater. Chem*., 2010, **20**, 2056–2062.
18 D. R. MacFarlane, J. Huang and M. Forsyth, *Nature*, 1999, **402**, 792–794.
19 P-J, Alarco, Y. Abu-Lebdeh, A. Abouimrane and M. Armand, *Nat. Mater*., **2004**, 3, 476-481.
20 J. S. Luo, A. H. Jensen, N. R. Brooks, J. Sniekers, M. Knipper, D. Aili, Q. F. Li, B. Vanroy, M. Wübbenhorst, F. Yan, L. V. Meervelt, Z. G. Shao, J. H. Fang, Z-H. Luo, D. E. De Vos, K. Binnemans and J. Fransaer, *Energy Environ. Sci*., 2015, **8**, 1276-1291.
21 P. Wang, Q. Dai, S. M. Zakeeruddin, M. Forsyth, D. R. MacFarlane and M. Grätzel, *J. Am. Chem. Soc*., 2004, **126**, 13590-13591.
22 H. Wang, X. Zhang, F. Gong, G. Zhou and Z. S. Wang, *Adv. Mater*., 2012, **24**, 121-124.
23 H. Wang, J. Li, F. Gong, G. Zhou and Z. S. Wang, *J. Am. Chem. Soc*., 2013, **135**, 12627-12633.
24 S. C. Li, L. H. Qiu, C. Z. Shi, X. J. Chen and F. Yan, *Adv. Mater*., 2014, **26**, 1266-1271.
25 G. W. Gokel, W. M. Leevy and M. E. Weber, *Chem. Rev*., 2004, **104**, 2723-2750.
26 C. J. Pedersen, *J. Am. Chem. Soc*., 1967, **89**, 7017-7036.
27 R. E. A. Dillon, C. L. Stern and D. F. Shriver, *Chem. Mater*., 2000, **12**, 1122-1126.
28 M. K. Kim, C. S. Lim, J. T. Hong, J. H. Han, H.-Y. Jang, H. M. Kim and B. R. Cho, *Angew. Chem. Int. Ed*., 2010, **49**, 364–367.
29 J. Fresneda, E. de Jesús, P. Gómez-Sal and C. L. Mardomingo, *Eur. J. Inorg. Chem*., 2005, 1468–1476.
30 A. A. El-Azhary and A. A. Al-Kahtani, *J. Phys. Chem. A*, 2005, **109**, 8041-8048.
31 A. Casnati, S. Barboso, H. Rouquette, M-J. Schwing-Weill, F. Arnaud-Neu, J-F. Dozol and R. Ungaro, *J. Am. Chem. Soc*., 2001, **123**, 12182-12190.
32 C. W. Shi, S. Y. Dai, K. J. Wang, X. Pan, L. Guo, L. H. Hu and F. T. Kong, *Chin. J. Chem*., 2005, **23**, 251-254.
33 Z. Huo, S. Dai, K. Wang, F. Kong, C. Zhang, X. Pan and X. Fang, *Sol. Energy Mater. Sol. Cells,* 2007, **91**, 1959-1965.
34 S. Cong, Y. Wang, Q. Yi, J. Zhao, Y. Sun, M. Shen and G. Zou. *J. Mater. Chem. A*, 2014, **2**, 20147-20153.
35 H. X. Wang, J. Bel, J. Desilvestro, M. Bertoz and G. Evans, *J. Phys. Chem. C*, 2007, **111**, 15125-15131.
36 C. Capiglia, P. Mustarelli, E. Quartarone, C. Tomasi and A. Magistris, *Solid State Ionics*., 1999, **118**, 73-79.
37 P. Wang, Q. Dai, S. M. Zakeeruddin, M. Forsyth, D. R. MacFarlane and M. Grätzel, *J. Am. Chem. Soc*., 2004, **126**, 13590-13591.
38 Y. Wang, P. F. Sun, S. Cong, J. Zhao and G. F. Zou, *Carbon*, 2015, **92**, 262-270.
39 Y. Zhao, J. Zhai, J. L. He, X. Chen, L. Chen, L. P. Zhang, Y. X. Tian, L. Jiang and D. B. Zhu, *Chem. Mater*., 2008, **20**, 6022-6028.
40 C. P. Lee, M. H. Yeh, R. Vittal and K. C. Ho, *J. Mater. Chem*., 2011, **21**, 15471-15478.
41 C. P. Lee, M. H. Yeh, R. Vittal and K. C. Ho, *J. Mater. Chem*., 2011, **21**, 15471-15478.
42 H. Wang, X. Zhang, F. Gong, G. Zhou and Z. S. Wang, *Adv. Mater*., 2012, **24**, 121–124.

Graphical Abstract

A novel solid-state electrolyte based on crown ether lithium salt complex

Minda Gao, Yun Wang, Qinghua Yi, Ying Su, Pengfei Sun, Xiangguo Wang, Jie Zhao* and Guifu Zou*

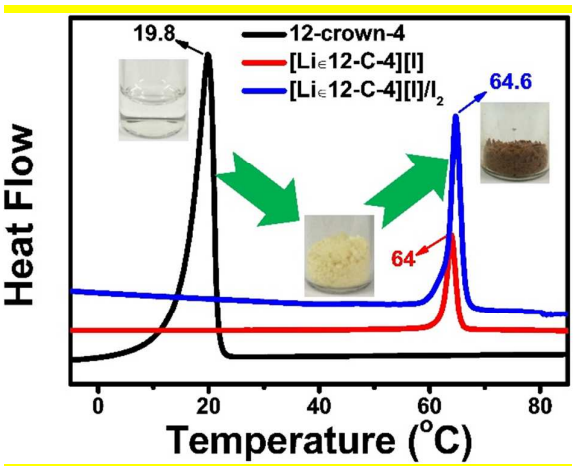

A novel solid-state electrolyte based on crown ether lithium salt complex [Li∈12-C-4][I] has been designed, synthesized and characterized.